Available online at www.scholarsresearchlibrary.com

Scholars Research Library

Der Pharmacia Lettre, 2020, 12 (3): 15-21
(http://scholarsresearchlibrary.com/archive.html)

ISSN 0975-5071
USA CODEN: DPLEB4

Potential Inhibiting Activities of 1,2,3-Triazole-Pyrimidine Hybrids (1,2,3-Tph) Against Focal Adhesion Kinase Reducing Skin Cancer Growth

Oyebamiji AK[1,2*], Alice AB[1], Aremu AO[2], Semire B[2]

[1]*Department of Basic Sciences, Faculty of Science, Adeleke University, P.M.B. 250, Ede, Osun State, Nigeria.*

[2]*Computational Chemistry Laboratory, Department of Pure and Applied Chemistry, Ladoke Akintola University of Technology, P.M.B. 4000, Ogbomoso, Oyo State, Nigeria.*

[*]***Corresponding author:*** *Oyebamiji AK, Department of Basic Sciences, Faculty of Science, Adeleke University, P.M.B. 250, Ede, Osun State, Nigeria. E-mail: abeloyebamiji@gmail.com*

ABSTRACT

The war declared by several researchers over skin cancer have been is becoming fierce globally. Eighteen molecular compounds were optimized using quantum chemical methods and many effective molecular descriptors EHOMO (eV), ELUMO (eV), dipole moment (Debye), log P, molecular weight (amu), HBA, HBD, Vol and Ovality) were obtained. The obtained descriptors were screened and used to develop efficient QSAR model using Gretl. The developed QSAR model predicted the observed inhibition concentration well. Also, non-bonding interaction between the studied compounds and focal adhesion kinase (PDB ID: 1mp8) were observed via docking studies. Compound 2 with -9.6 kcal/mol possess the ability to inhibit than other studied compounds; the studied compounds have the ability to inhibit than the standard used (5FU).

Keywords: 1,2,3-triazole-pyrimidine hybrids (1,2,3-TPH), Focal Adhesion Kinase, Skin Cancer, QSAR, DFT

INTRODUCTION

The battle against skin cancer by scientists over the world has increased for decades. The rate at which this malignant melanoma increases is faster than any other type of cancer [1,2]. In America, information showed that one (1) out of six (6) have malignant melanoma in their days [3,4]. This type of cancer is one of the existing cancers that can be prevented from occurring.

Skin cancer is mostly caused by some eco-friendly agents like UV radiation, chemicals, micro-organism that can cause disease, as well as temperature variations [5].

Accumulation of these agents in human bodies led to skin cancer and active molecular chemical compounds have been one of the ways to terminate skin cancer development in human body [6]. Moreover, in many types of cancer, focal adhesion kinase is mostly overexpressed and triggered [7,8]. Also, focal adhesion kinase is restricted to focal adhesion and it is prompted through extracellular indications. More so, it roles in the interaction within human cells are vital [9].

Reports have shown that triazoles and pyrimidines are vital drug-like compounds in medicinal world. Several scientists have reported that both triazoles and pyrimidines have much biological importance like anticancer, anti-inflammatory, analgesics, antioxidant, and diuretics [10-18].

So, hybrids of triazole and pyrimidine are expected to possess more proficient biological importance than either of the two compounds. Thus, the aim of this work is to examine the interactions existing between the studied compounds (Table 1) and focal adhesion kinase (PDB ID: 1mp8) as well as developing effective QSAR model using 3D-descriptors obtained from the optimization of the studied compounds. The name of the studied compounds are 2-((1-(2-chlorobenzyl)-1H-1,2,3-triazol-4-yl)methylthio)-4-((4-methoxyphenyl)amino)-6-phenylpyrimidine-5-carbonitrile(1), 2-((1-(2-chlorobenzyl)-1H-1,2,3-triazol-4-yl)methylthio)-4-phenyl-6-((3-(trifluoromethyl)phenyl)amino)pyrimidine-5-carbonitrile(2), 2-((1-(2-chlorobenzyl)-1H-1,2,3-triazol-4-yl)methylthio)-4-((2-chlorophenyl)amino)-6-phenylpyrimidine-5-carbonitrile(3), 2-((1-(2-chlorobenzyl)-1H-1,2,3-triazol-4-yl)methylthio)-4-((4-chlorophenyl)amino)-6-phenylpyrimidine-5-carbonitrile(4), 2-((1-(2-chlorobenzyl)-1H-1,2,3-triazol-4-yl)methylthio)-4-((3-chlorophenyl)amino)-6-phenylpyrimidine-5-carbonitrile(5), 2-((1-(2-chlorobenzyl)-1H-1,2,3-triazol-4-yl)methylthio)-4-((2-methoxyphenyl)amino)-6-phenylpyrimidine-5-carbonitrile(6), 2-((1-(2-chlorobenzyl)-1H-1,2,3-triazol-4-yl)methylthio)-4-((2-fluorophenyl)amino)-6-phenylpyrimidine-5-carbonitrile(7), 2-((1-(2-chlorobenzyl)-1H-1,2,3-triazol-4-yl)methylthio)-4-((4-fluorophenyl)amino)-6-phenylpyrimidine-5-carbonitrile(8), 2-((1-(2-chlorobenzyl)-1H-1,2,3-triazol-4-yl)methylthio)-4-phenyl-6-(o-tolylamino)pyrimidine-5-carbonitrile(9), 2-((1-(4-fluorobenzyl)-1H-1,2,3-triazol-4-yl)methylthio)-4-phenyl-6-(p-tolylamino)pyrimidine-5-carbonitrile(10), 2-((1-(4-methylbenzyl)-1H-1,2,3-triazol-4-yl)methylthio)-4-phenyl-6-(p-tolylamino)pyrimidine-5-carbonitrile(11), 4-((2-fluorophenyl)amino)-2-((1-(4-methylbenzyl)-1H-1,2,3-triazol-4-yl)methylthio)-6-phenylpyrimidine-5-carbonitrile(12), 2-((1-(2-chlorobenzyl)-1H-1,2,3-triazol-4-yl)methylthio)-4-phenyl-6-(p-tolylamino)pyrimidine-5-carbonitrile(13), 2-((1-(2-chlorobenzyl)-1H-1,2,3-triazol-4-yl)methylthio)-4-(4-isopropylphenyl)-6-(p-tolylamino)pyrimidine-5-carbonitrile(14), 2-((1-(2-chlorobenzyl)-1H-1,2,3-triazol-4-yl)methylthio)-4-(4-isopropylphenyl)-6-(p-tolylamino)pyrimidine-5-carbonitrile(15), 2-((1-(2-chlorobenzyl)-1H-1,2,3-triazol-4-yl)methylthio)-4-(p-tolyl)-6-(p-tolylamino)pyrimidine-5-carbonitrile(16), 2-((1-(2-chlorobenzyl)-1H-1,2,3-triazol-4-yl)methylthio)-4-(4-chlorophenyl)-6-(p-tolylamino)pyrimidine-5-carbonitrile(17), 4-(4-bromophenyl)-2-((1-(2-chlorobenzyl)-1H-1,2,3-triazol-4-yl)methylthio)-6-(p-tolylamino)pyrimidine-5-carbonitrile(18).

Table 1: Structures of 1,2,3-triazole-pyrimidine hybrids.

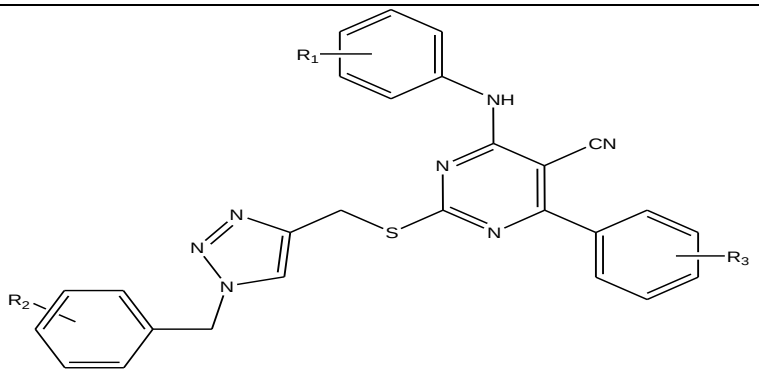

Compound	R_1	R_2	R_3
1.	*p*-OCH_3	*o*-Cl	H
2.	*m*-CF_3	*o*-Cl	H
3.	*o*-Cl	*o*-Cl	H
4.	*p*-Cl	*o*-Cl	H
5.	*m*-Cl	*o*-Cl	H
6.	*o*-OCH_3	*o*-Cl	H
7.	*o*-F	*o*-Cl	H
8.	*p*-F	*o*-Cl	H
9.	*o*-CH_3	*o*-Cl	H
10.	*p* -CH_3	*p*-F	H
11.	*p* -CH_3	*p* -CH_3	H
12.	*o*-Cl	*p* -CH_3	H
13.	*p* -CH_3	*o*-Cl	H
14.	*p* -CH_3	*o*-Cl	*p*-$CH(CH_3)_2$
15.	*o*-OCH_3	*o*-Cl	*p*-$CH(CH_3)_2$
16.	*p* -CH_3	*o*-Cl	*p* -CH_3
17.	*p* -CH_3	*o*-Cl	*p*-Cl
18.	*p* -CH_3	*o*-Cl	*p*-Br

RESEARCH METHODOLOGY

Optimization, quantitative structural activities relationship (QSAR) and docking studies were carried out on 1,2,3-triazole-pyrimidine hybrids. Many efficient parameters (volume, ovality, polarizability, EHOMO, ELUMO, Bandgap) were obtained from the optimization of the studied compounds using B3LYP with 6-31+G* as basis set. The selected descriptors were used to develop proficient QSAR model using multiple linear regression (MLR) via Gretl [19] software. More so, the validation of the developed QSAR model was accomplished through cross validation (CV. R2) (equation 1), adjusted squared correlation coefficient (R_a^2) (equations 2) and p-value [20]. Furthermore, the prediction of principal binding mode of drug-like molecules together with the receptor of identified three-dimensional structure was calculated using docking approach. Pymol v1.74, Auto Dock Tools 1.5.6, Auto Dock Vina programmed and Discovery Studio R2 was used as post-dock software for viewing the interaction between the ligand and the receptor. Calculated inhibition constant was achieved via equation 3.

$$\boldsymbol{CV.R^2 = 1 - \frac{\sum(Y_{obs} - Y_{cal})^2}{\sum(Y_{obs} - \bar{Y}_{obs})^2}} \qquad \textbf{(1)}$$

$$\boldsymbol{R_a^2 = \frac{(N-I)\times R^2 - P}{N-1-P}} \qquad \textbf{(2)}$$

$$K_i = e^{-\Delta G/RT} \quad (3)$$

Note: ΔG = binding affinity (Kcal/mol), gas constant (R) = 1.987 (cal/mol/K) and absolute temperature (T) = 298.15.

RESULTS AND DISCUSSION

Biological activities of eighteen molecular compounds were explored via quantitative structure activity relationship and molecular docking study. The characteristics of the developed QSAR model are expressed by its correlation coefficient which signifies the fitness of the calculated inhibition concentration to the observed inhibition concentration.

QSAR Study on 1,2,3-Triazole-Pyrimidine Hybrids (1,2,3-TPH)

Eighteen molecular compounds were considered for biological study in this work. The entire compounds were divided in to two i.e. training set (11 compounds) and test set (7 compounds). The selected compounds used as training set was used in making QSAR model while the selected compounds were used as test set for assessing the predicting power of the developed QSAR model. Also, low residual value is obtained for the calculated inhibition concentration using equation 4 and this show that the developed QSAR model has a good ability to predict. Moreover, the descriptive analysis features for both training set and test set as shown in Table 2 display similarity in biological activity of two datasets and this could be due to closeness between the values for training set and test set (Tables 3 and 4).

$$IC_{50} = 21224.3 + 41.5429(Vol) + 66.667(Ovality) – 513.324(Polar) - 132.673(BG) \quad (4)$$

Table 2: Descriptive analysis of 1,2,3-Triazole-Pyrimidine Hybrids (1,2,3-TPH).

Descriptive Values	Training Set	Test Set
Dataset Number	11.00	7.00
Mean dependent var	4.33	4.70
S.D. dependent var	2.06	2.27
S.E. of regression	1.22	0.94
Mean Squared Error	0.81	0.25
Theil's U	0.27	0.15
F = 5.620840, P < 0.0001, R2 = 0.789, R_adj^2 = 0.648, CV. R2 = 0.903, MSE = 0.817		

Furthermore, validation of the calculated analysis using multiple linear regression (MLR) was accomplished by considering cross validation ($CV.R^2$), adjusted correlation coefficient (R_a^2), mean square error (MSE) and p-value. This was examined for confirming the power and dependability of the developed QSAR model, since correlation coefficient is not only enough to determine the effectiveness of the developed QSAR model (Table 3). Therefore, the facts shown in Table 3 have proved that the predicting strength of the developed QSAR model is reliable.

Table 3: Standard value for QSAR model validation.

QSAR model validation parameters	Standard value	Developed QSAR model value	Comments
Correlation coefficient (R^2)	≥0.5	0.789	Pass
Adjusted Correlation coefficient ($\boldsymbol{R_a^2}$)	≥0.6	0.648	Pass
Cross validation coefficient ($CV.R^2$)	≥0.5	0.903	Pass
Confidence interval at 95% confidence level (P-value)	<0.05	0.031	Pass

Table 4: Experimental and calculated inhibition concentration.

Variables	Observed IC_{50}	Calculated IC_{50}
1*	3.99	7.16
2	3.71	2.55
3*	8.35	7.60
4	1.59	3.02
5	3.59	3.02
6	7.86	8.03
7*	5.23	4.19
8	5.34	4.52
9*	2.76	1.59
10	3.04	4.71
11	8.16	7.09
12*	7.08	3.73
13	3.39	2.94
14	3.53	4.18
15	2.69	2.48
16*	2.63	3.23
17	4.81	4.83
18*	2.87	4.00

Docking results

The docking results of the studied complex were displayed in term of binding affinity as shown in Table 5. In this work, series of non-bonding interaction were observed between 1,2,3-Triazole-Pyrimidine Hybrids (1,2,3-TPH) and focal adhesion kinase with PDB ID 1mp8. The effect of the substituents attached were obvious both in the conformation of each of the complex and the in the calculated binding affinity. Compound 2 with binding affinity value of -9.6 proved to possess the utmost ability to inhibit focal adhesion kinase since it was proved by Oyebamiji et al., 2020 that compound with lowest binding affinity have the greater tendency to inhibit than other studied compounds [21]. Therefore, compound 2 have the higher tendency to inhibit that other compounds studied in this work and this was agreed to be a function of CF3 attached to meta position of the benzene tagged R1 (Figure 1) (Table 5).

The inhibition constant for each of the compound was displayed in Table 5. More so, all the studied compounds were observed to poses higher ability to inhibit focal adhesion kinase than the standard drug used in this work.

Table 5: The molecular docking result obtained from **1,2,3-TPH** and 1mp8

Comp	Scoring (kcal/mol)	K (µM)
1.	-8.2	1.02×10^{6}
2.	-9.6	1.09×10^{7}
3.	-8.6	2.01×10^{6}
4.	-9.0	3.96×10^{6}
5.	-8.6	2.01×10^{6}
6.	-8.6	2.01×10^{6}
7.	-8.8	2.82×10^{6}
8.	-8.8	2.82×10^{6}

9.	-8.6	2.01×10^6
10.	-8.9	3.34×10^6
11.	-8.9	3.34×10^6
12.	-8.6	2.01×10^6
13.	-8.7	2.38×10^6
14.	-9.3	6.57×10^6
15.	-9.0	3.96×10^6
16.	-8.5	1.70×10^6
17.	-8.8	2.82×10^6
18.	-8.8	2.82×10^6
5FU	-4.7	2.78×10^3

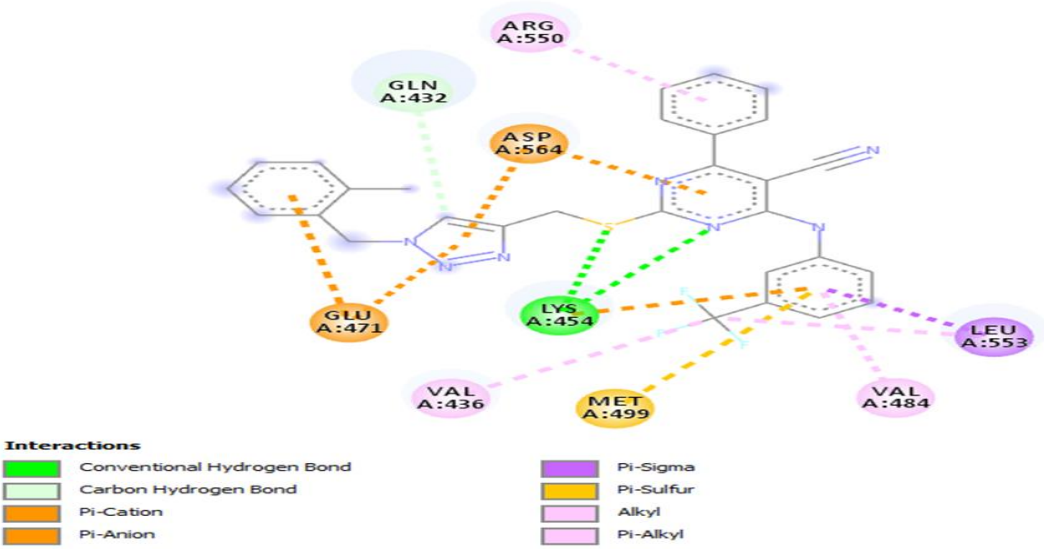

Figure 1: Binding interaction between compound 2 and 1 mp8.

CONCLUSION

In this work, the optimized compounds were used to develop QSAR model for better prediction of the observed studied compounds. The developed QSAR model proved to be effective since the predicted bioactivity were closer to the observed bioactivity. The QSAR model were validated by considering CVR2, adjusted R2, and P-value and it was confirmed that the developed model possesses the ability to predict well. Also, all the studied compounds showed a better ability to inhibit than the standard used in this work. More so, compound 2 possess more efficiency to inhibit than other studied compounds.

REFERENCES

[1]. Arrangoiz, R., et al., Melanoma review: Epidemiology, risk factors, diagnosis and staging. *J Cancer Treat Research*. 2016.4: P.1-15.

[2]. Karimkhani, C., et al., The global burden of melanoma: results from the Global Burden of Disease Study 2015. *Br J Dermatol*. 2017.177:134-140.

[3]. Javed, I., et al., Potential phytochemicals in the fight against skin cancer: Current landscape and future perspectives. *Biomed Pharmacother*. 2019.109:1381-1393.

[4]. Randy, M.G., Skin cancer: More than skin deep. *Adv Skin Wound Care*.2009.22:574-580.

[5]. Penta, D., Somashekar, BS., Meeran, SM., Epigenetics of skin cancer: Interventions by selected bioactive phytochemicals. Photodermatol Photoimmunol. *Photomed*. 2018.3(1):42-49.

[6]. Amawi, H., Ashby, C.R., Tiwari, A.K., Cancer chemoprevention through dietary flavonoids: what's limiting?. *Chin J Cancer*.2017.36:50.

[7]. Frank, A.N., Vanderputten, M., and Ocak, S., Role of Focal Adhesion Kinase in Small-Cell Lung Cancer and Its Potential as a Therapeutic Target. *Cancers*. 2019.11:1683.

[8]. Ocak, S., et al., DNA copy number aberrations in small-cell lung cancer reveal activation of the focal adhesion pathway. *Oncogene*. 2010.29:6331-6342.

[9]. Schaller, MD., Borgman, CA., Parsons, J.T. Autonomous expression of a noncatalytic domain of the focal adhesion-associated protein tyrosine kinase pp125FAK. *Mol Cell Biol*. 1993.13:785-791.

[10]. Bo, Z., Human 3α-hydroxysteroid dehydrogenase type 3: structural clues of 5α-DHT reverse binding and enzyme down-regulation decreasing MCF7 cell growth. *Biochem* J. 2016.473:1037-1046.

[11]. Virginie, N., et al., Structure of the Human 3α-Hydroxysteroid Dehydrogenase Type 3 in Complex with Testosterone and NADP at 1.25-Å Resolution. *J BioChem*. 2001.276:42091-42098.

[12]. Basu, Nk and Rose, FL., 1081. S-triazolopyridazines: Synthesis as potential therapeutic agents. *J Chem Soc*.1963. 5660.

[13]. El-Dawy, MA., Hozzoa, AB., Synthesis of some new 1,2,4-triazole derivatives. *J Pharm Sci*. 1983.72:45.

[14]. Mishra, A., et al., Search for new pharmacophores for antimalarial activity. Part III: synthesis and bioevaluation of new 6-thioureido-4-anilinoquinazolines. *Eur J Med Chem*. 2009.44:4404-4412.

[15]. Wu, J., et al., Prognostic role of LSD1 in various cancers: Evidence from a meta-analysis. *OncoTargets Ther*. 2015.8:2565-2570.

[16]. Lazrak, F., et al., Bond lengths and bond orders in π-electron heterocycles. *Phosphorus, Sulfur, and Silicon*.1792.004:1799-1808.

[17]. Lazrak, F., et al., Inhibiting Activity of 1,2,3-TriazolePyrimidine-Urea Hybrids Against Esophageal Cancer: Theoretical Approach. *Indian J Chem Orga Medi Chem*. 2002.41.821-825.

[18]. Kumar, H., et al., 1,3,4-Oxadiazole/thiadiazole and 1,2,4-triazole derivatives of biphenyl-4-yloxy acetic acid: synthesis and preliminary evaluation of biological properties. *Eur J Med Chem*. 2008.43:2688-2698.

[19]. http://gretl.sourceforge.net/

[20] Ghamali, M., et al., QSAR analysis of the toxicity of phenols and thiophenols using MLR and ANN. *J Taibah Univ Sci*. 2017.11:1-10.

[21] Oyebamiji, A.K., Semire, B., *In vitro* biological estimation of 1,2,3-Triazolo[4,5-d] pyrimidine derivatives as anti-breast cancer agent: DFT, QSAR and docking studies. *Curr Pharm Biotechnol*. 2020.21:70-78.